Modification at a boron unit: tuning electronic and optical properties of π-conjugated acyclic anion receptors†

Hiromitsu Maeda,*[a,b] Mayumi Takayama,[a] Kazuki Kobayashi[c] and Hideyuki Shinmori[c]

Received 26th April 2010, Accepted 17th June 2010
DOI: 10.1039/c0ob00044b

Substituents at the boron unit of dipyrrolyldiketone boron complexes as π-conjugated acyclic anion receptors play crucial roles for the tuning of solid-state molecular assemblies, anion-binding behaviour and electronic and optical properties. In particular, emission quantum yields can be significantly tunable by boron substituents and pyrrole α-aryl moieties.

Introduction

π-Conjugated systems responsive to external chemical stimuli offer fascinating possibilities as building subunits of tunable electronic and optical materials. Modifications of the molecular structures are crucial for controlling their electronic and optical properties. As examples of stimuli-responsive π-conjugated molecules, we have reported highly emissive BF_2 complexes of 1,3-dipyrrolyl-1,3-propanediones (*e.g.*, **1a–d**), which efficiently bind anions as chemical stimuli[1,2] to induce the conformation changes with the inversion of pyrrole rings (Fig. 1).[3–6] Introduction of appropriate substituents at the pyrrole rings enables the acyclic anion receptors to form various anion-responsive supramolecular organized structures such as crystals, gels[5a] and amphiphilic vesicles.[5d] Another modification of the receptor structures can be achieved by the replacement of fluorine units in BF_2 complexes, which affords catechol-boron-substituted 'BO_2' complexes such as **2a**,**b**; these molecules are less emissive than **1a**,**b**.[6] Therefore, in order to examine the effects of B-substituents for their electronic and optical properties, we have introduced less electronegative 'carbon' moieties—phenyl rings in this case—at the boron unit to provide 'BC_2' complexes. Singlet oxygen generation can also be controlled by anion complexation.

Results and discussion

BC_2 complexes, diphenylboron-substituted derivatives **3a–c**, were synthesized in 71, 66 and 66% yield by the treatment of the corresponding diketones with BPh_3.[7] Similar to **1d**,[5b] β-ethyl **3d** was obtained in 9.0% yield by the iodination of **3b** and following it up with a coupling reaction with phenylboronic acid. On the other hand, by following the procedures mentioned in literature

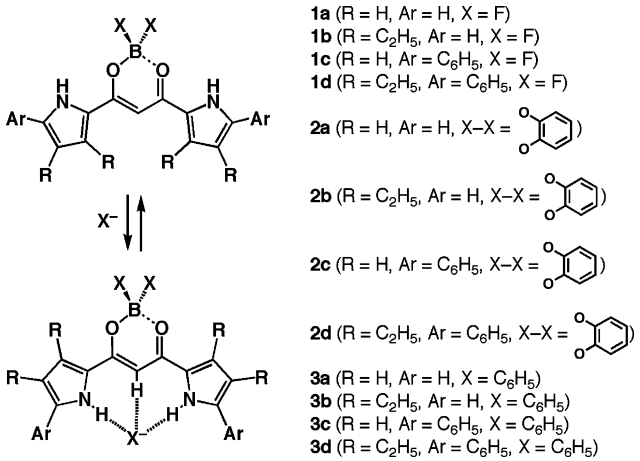

Fig. 1 Anion-binding scheme of dipyrrolyldiketone boron complexes as π-conjugated acyclic anion receptors **1a–d**, **2a–d** and **3a–d**.

for **2a**,**b**,[6] α-phenyl-substituted BO_2 complex **2c** was obtained as a reference molecule in 80% yield from diketone by treatment with BCl_3 and catechol. In addition, similar to **1d** and **3d**, β-ethyl **2d** was synthesized in 3.5% yield from **2b**,[6] which was the starting material. Chemical identification of these compounds was carried out by ^{1}H NMR and MALDI-TOF-MS. ^{11}B NMR of **3b** in $CDCl_3$ at 20 °C exhibits a broad signal at 8.09 ppm in contrast to the fairly sharp signals of **1b** (0.44 ppm) and **2b** (8.45 ppm).

Photophysical data are summarised in Table 1. UV/vis absorption maxima (λ_{max}) of β-ethyl **1b**, **2b** and **3b** in CH_2Cl_2 are 451, 455 and 448 nm, respectively, whereas those of α-phenyl **1d**, **2d** and **3d** are observed at 499, 502 and 489 nm, respectively; these λ_{max} values suggest that substituents at boron units slightly affect the energy gaps between the ground and excited states. Similarly, λ_{max} values of **1a**, **2a** and **3a** in CH_2Cl_2 are 432, 435 and 435 nm, respectively, and those of α-phenyl **1c**, **2c** and **3c** are 500, 503 and 492 nm, respectively. Energy levels of HOMO/LUMO corresponding to the MO located on receptor units estimated by DFT calculations are, for example, –5.798/–2.714 eV for **1c**, –5.160/–2.745 eV for **2c** and –5.714/–2.628 eV for **3c**, which are correlated with the electron-withdrawing and electron-donating properties of boron-substituents.[8]

In contrast to fairly small distinctions in absorption, interestingly, emission properties such as quantum yields (Φ_F) excited at each λ_{max} can be dramatically controlled by boron substituents (Table 1): for example, Φ_F values (and λ_{em}) of **1b**, **2b** and **3b** are

[a]*College of Pharmaceutical Sciences, Institute of Science and Engineering, Ritsumeikan University, Kusatsu, 525-8577, Japan. E-mail: maedahir@ph.ritsumei.ac.jp; Fax: +81 77 561 2659; Tel: +81 77 561 5969*
[b]*PRESTO, Japan Science and Technology Agency (JST), Kawaguchi, 332-0012, Japan*
[c]*Division of Medicine and Engineering Science, Interdisciplinary Graduate School of Medical and Engineering, University of Yamanashi, Kofu, 400–8511, Japan*

† Electronic supplementary information (ESI) available: Anion-binding behaviour and CIF files for the X-ray structural analysis of **2d**, **3a,b**, **3b-I$_2$**, **3c**, **3c**·acetone$_2$, **3d**, **3a–c**·TBABr and **3d**·TBACl. CCDC reference numbers 759617–759627. For ESI and crystallographic data in CIF or other electronic format see DOI: 10.1039/c0ob00044b

Table 1 Photophysical data (absorption maximum λ_{max} (nm), fluorescence emission maximum λ_{em} (nm), emission quantum yield Φ_F, and fluorescence lifetime τ (ns)) of **1a–d**, **2a**,**b** (references), **2c**,**d** and **3a–d** in CH_2Cl_2[a]

	λ_{max}/nm	λ_{em}/nm	Φ_F	τ/ns
1a	432 [a]	451 [a]	0.96	—
1b	451 [b]	470 [b]	0.98 [b]	0.74 (10%), 2.32 (88%)
1c	500 [c]	529 [c]	0.95	—
1d	499 [d]	535 [d]	0.94 [d]	0.98 (16%), 2.24 (78%)
2a	435 [e]	450 [e]	0.003	—
2b	455 [e]	474 [e]	0.001	0.14 (0.023%), 2.17 (0.077%)
2c	503	530	0.002	—
2d	502	537	0.003	0.73 (0.18%), 1.60 (0.12%)
3a	435	449	0.009	—
3b	448	464	0.072	0.23 (3.7%), 2.04 (3.5%)
3c	492	517	0.87	—
3d	489	512	0.94	0.70 (11%), 2.13 (83%)

[a] Ref. 4*a*. [b] Ref. 4*b*. [c] Ref. 5. [d] Ref. 5*b*. [e] Ref. 6

0.98 (470 nm), 0.001 (474 nm) and 0.072 (464 nm), respectively, and those of **1d**, **2d** and **3d** are 0.94 (535 nm), 0.003 (537 nm) and 0.94 (512 nm), respectively. β-Unsubstituted receptors exhibit the similar tendency: Φ_F values (and λ_{em}) of **1a**, **2a** and **3a** are 0.96 (451 nm), 0.003 (450 nm) and 0.009 (449 nm), whereas those of **1c**, **2c** and **3c** are 0.95 (529 nm), 0.002 (530 nm) and 0.87 (517 nm). These results suggest that the excited states and quenching processes of diphenylboron-substituted **3a–d** are significantly affected by α-phenyl-substituents, which enhance Φ_F values; this is in sharp contrast to the highly emissive BF_2 complexes **1a–d** and the less emissive catechol-boron **2a–d**, regardless of whether the receptors have α-phenyl moieties or not (Fig. 2). As speculated from theoretical studies, one of the quenching processes is presumably intramolecular electron transfer between core π-units and aryl moieties around the boron. Further, fluorescence lifetimes (τ, ns) by excitation at 399.5 nm (and contributions for emission efficiencies based on the Φ_F values excited at each λ_{max}) are 0.74 (10%) and 2.32 (88%) for **1b**, 0.98 (16%) and 2.24 (78%) for **1d**, 0.14 (0.023%) and 2.17 (0.077%) for **2b**, 0.73 (0.18%) and 1.60 (0.12%) for **2d**, 0.23 (3.7%) and 2.04 (3.5%) for **3b** and 0.70 (11%) and 2.13 (83%) for **3d**. The relatively larger contributions of shorter lifetimes in **2b**,**d** and **3b** are correlated with their lesser emissive properties.

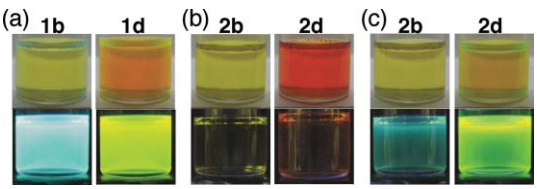

Fig. 2 Photographs of the CH_2Cl_2 solutions (1×10^{-3} M, under visible (top) and $UV_{365\,nm}$ (bottom) light) of (a) **1b** and **1d**, (b) **2b** and **2d** and (c) **3b** and **3d**.

Single-crystal X-ray analyses of **3a–d** elucidated the exact structures of the BC_2 complexes and their molecular assemblies in the solid state (Fig. 3). In these receptors, one of the B-phenyl rings is tilted almost perpendicular to the core plane, as also observed in the DFT-based optimized structures. Focusing on the assemblies, β-unsubstituted **3a** forms dimers by fairly weak edge-to-edge stacking (3.74 Å) along with the dimeric structures

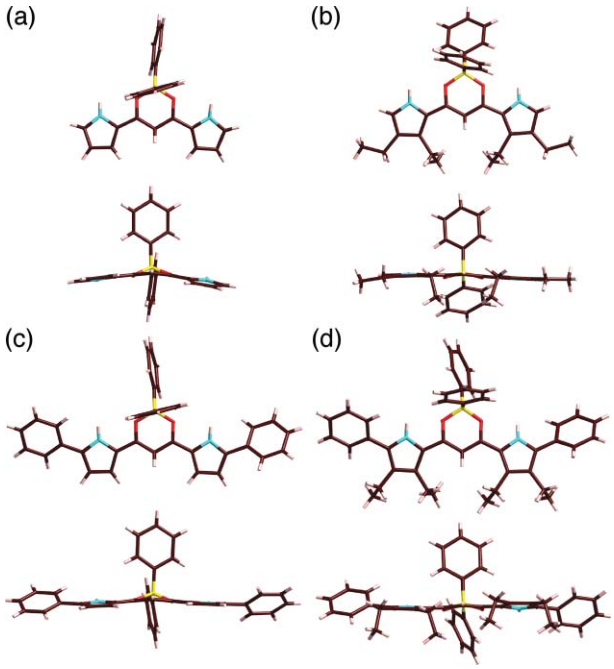

Fig. 3 Single-crystal X-ray structures (top and side view) of (a) **3a**, (b) **3b** (one of the two independent structures), (c) **3c** (one of the two independent structures) and (d) **3d**. Atom colour code: brown, pink, yellow, blue, and red refer to carbon, hydrogen, boron, nitrogen and oxygen, respectively.

by N–H···phenyl-π interaction (N···π: 3.35 Å), whereas β-ethyl **3b** exhibits 1-D ordered structures along the *b* axis and π–π interaction (3.61 Å) between the 1-D columns. α-Phenyl **3c**, whose two phenyl moieties are tilted at 23.5° and 38.1° to the core π-plane, forms edge-to-edge stacking dimers (3.48 Å). Further, **3d** shows the phenyl ring tilts at 38.6° and 45.5° and forms stacking dimer structures at a distance of 3.77 Å, whose regular conformation is in sharp contrast to the corresponding BO_2 complex **2d** with an inverted pyrrole ring.

Next, anion-binding behaviour was examined. ^{1}H NMR spectral changes of, for example, **3c** in CD_2Cl_2 (1 mM) at −50 °C upon the addition of Cl^- as a tetrabutylammonium (TBA) salt (0 to 1.7 equiv) exhibited down-field shifts of pyrrole NH (9.83 to 12.32 ppm), *o*-CH (7.66 to 8.15 ppm) and bridging CH (6.53 to 8.58 ppm). This result suggests the formation of receptor–anion complexes in BC_2 complexes as well, as described in Fig. 1. The exact structures of receptor–anion complexes were revealed by single-crystal X-ray analyses of **3a**·TBABr, **3b**·TBABr, **3c**·TBABr and **3d**·TBACl (Fig. 4). In these cases, two pyrrole rings are inverted to afford receptor–anion complexes; for example, in **3c**·TBABr, the N(–H)···Br^-, bridging-C(–H)···Br^- and *o*-C(–H)···Br^- distances are 3.27/3.31, 3.48 and 3.54/3.62 Å, respectively, and the α-phenyl moieties are tilted to the core π-plane at 8.71° and 29.04°, which are much smaller than those of **3c**. In this case, the 'regular' binding mode in **3a**·TBABr is in sharp contrast to the anion-bridged 1-D chain structures of **1a**·TBACl[4a] and **1a**·TBABr.[5e] These differences in molecular conformation, correlated with their assembled structures, are due to the stable packing modes that are significantly affected by the shapes and bulkiness of B-substituents. Similar to the former examples,[5a,c] receptor–anion complexes are stacked with TBA cations to form columnar structures. Further, UV/vis spectra of **3a–d** along with

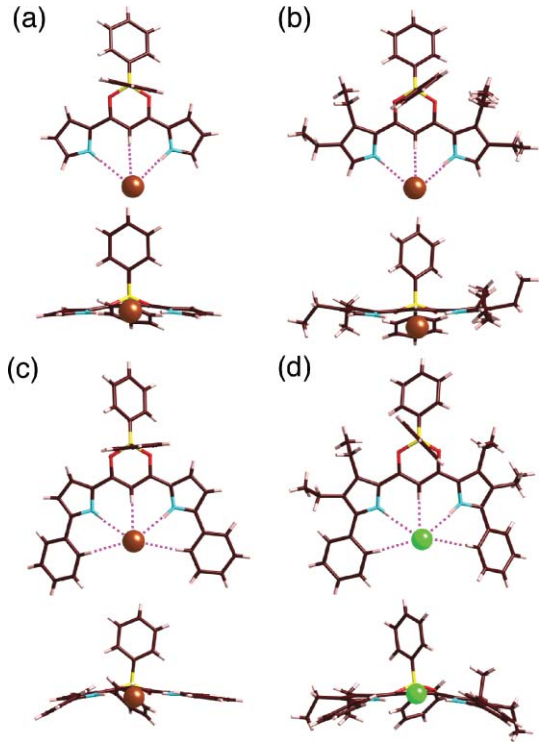

Fig. 4 Single-crystal X-ray structures (top and side view) of (a) **3a**·TBABr, (b) **3b**·TBABr, (c) **3c**·TBABr and (d) **3d**·TBACl. Counter cations are omitted for clarity. Atom colour code: red-brown and yellow-green refer to bromine and chlorine, respectively.

2c,**d** in CH_2Cl_2 are changed by anion complexation: for example, addition of TBACl to **3a**, **3b**, **3c** and **3d** in CH_2Cl_2 affords small decreases in absorption with almost no changes of λ_{max} values for **3a**, **3b** and **3c** and subtle shift (+4 nm) for **3d**. On the other hand, fluorescence spectral changes by anions are observed: for example, Cl^- binding of **3b** enhances fluorescence quantum yield to 0.40, in contrast to **3d**, which shows almost similar Φ_F value (0.83). Enhancement of the Φ_F value is possibly because of the changes in the molecular orbitals by anion binding. Binding constants (K_a) of the receptors for various anions in CH_2Cl_2 were examined by the UV/vis absorption spectral changes (Table 2). In the case of α-phenyl receptors (**1c**, **2c** and **3c**), BC_2 complex **3c** shows K_a values that are comparable to those of **1c** and **2c**. On the other hand, in the receptors bearing β-ethyl moieties (**1b**, **2b**, **3b**, **1d**, **2d** and **3d**), K_a values of **3b** and **3d** for halide anions are greater than those of the corresponding BF_2 and BO_2 complexes. Oxoanions such as $CH_3CO_2^-$ and $H_2PO_4^-$ are well bound by the receptors due to the basicities of anions. Detailed factors that go to determine the anion-binding affinities, especially related with B-substituents, are now being examined. Acyclic geometries of the receptor molecules exhibit the anion selectivities that are much affected by substituents.

Based on the optical properties of the receptors depending on the B-substituents and anion complexation, abilities to sensitize singlet oxygen ($^1O_2$) generation were examined by photoirradiation of anion receptors containing 1,3-diphenylisobenzofuran (DPBF), and this caused clear absorption spectral changes associated with DPBF oxidation.[9] In this case, α-phenyl β-ethyl receptors **1d**, **2d** and **3d** are used due to their solubility and appropriate

Table 2 Binding constants (K_a, M^{-1}) of **1a–d**, **2a**,**b** (references), **2c**,**d** and **3a–d** with various anions as TBA salts in CH_2Cl_2 [a]

	K_a (**1a**) [b]	K_a (**1b**) [c]	K_a (**1c**) [d]	K_a (**1d**) [e]	K_a (**2a**)	K_a (**2b**) [f]	K_a (**2c**)	K_a (**2d**)	K_a (**3a**)	K_a (**3b**)	K_a (**3c**)	K_a (**3d**)
Cl^-	15 000 [b]	6800 (0.45)	30 000 (2.0)	2700 (0.18)	5800 (0.39)	2300 (0.15)	19 000 (1.3)	410 (0.027)	18 000 (1.2)	23 000 (1.5)	13 000 (0.87)	3300 (0.22)
Br^-	2100 [b]	1200 (0.57)	2800 (1.33)	300 (0.14)	660 (0.31)	270 (0.13)	1600 (0.76)	90 (0.043)	940 (0.45)	3300 (1.6)	1200 (0.57)	350 (0.17)
$CH_3CO_2^-$	930 000 [b]	210 000 (0.23)	210 000 (0.23)	27 000 (0.029)	250 000 (0.27)	33 000 (0.035)	210 000 (0.23)	7, 400 (0.0080)	130 000 (0.14)	94 000 (0.10)	68 000 (0.073)	18 000 (0.019)
$H_2PO_4^-$	270 000 [b]	91 000 (0.34)	72 000 (0.27)	2200 (0.0081)	12 000 (0.044)	67 000 (0.25)	39 000 (0.14)	610 (0.0023)	9600 (0.036)	11 000 (0.041)	13 000 (0.048)	580 (0.0021)
HSO_4^-	640	1200 (1.9)	540 (0.84)	25 (0.039)	330 (0.52)	80 (0.13)	98 (0.15)	12 (0.019)	1700 (2.7)	3900 (6.1)	110 (0.17)	15 (0.023)

[a] The values in the parentheses are the ratios of the K_a values to the K_a value of **1a**. [b] Ref. 4*c*. [c] Ref. 4*b*. [d] Ref. 5*a*. [e] Ref. 5*b*. [f] Ref. 6

absorption bands that are less overlapped with that of DPBF. The $\lambda_{max}/\lambda_{em}$ values (nm) (and Φ_F) in toluene are comparable to those in CH_2Cl_2: 496/527 (0.97) for **1d**, 500/531 (0.001) for **2d** and 490/520 (0.91) for **3d**. Quantum yields (Φ_Δ) of $^1O_2$ formation for **1d**, **2d** and **3d** in toluene were determined to be 0.028, 0.029 and 0.065, respectively. Boron complexes exhibit $^1O_2$ generation abilities, and B-substituents such as diphenylboron can augment the efficiency. Less efficient generation of $^1O_2$ even in less emissive **2d** suggests that triplet state may not be the main fluorescent quenching pathway. Further, Cl^- complexes of **1d**, **2d** and **3d**, prepared by the addition of TBACl (35 equiv for samples in 10^{-6} M enough to obtain >90% Cl^- complexes) according to their K_a values in toluene, afford slightly increased Φ_Δ values of 0.068, 0.042 and 0.085, respectively. This result suggests that the photophysical properties can be controlled by external chemical stimuli.

Conclusions

Substituents at the boron unit of π-conjugated acyclic anion receptors have been found to modulate the electronic and optical properties, especially fluorescence efficiencies, along with solid-state assembled structures. Although we found the considerable differences in the derivatives with various B-substituents, we also noticed that the properties of these dipyrrolyldiketone boron complexes such as $^1O_2$ generation behaviour are tunable by anions. These properties observed in the anion receptors would be useful for efficient anion sensors and agents for photodynamic therapy (PDT) by further structure modifications. It is also essential to pointed out that, in contrast to fluorine moieties in BF_2 complexes, parent catechol and phenyl units in BO_2 and BC_2 complexes can be replaced by utility substituents and spacer units to afford supramolecular assemblies and covalently linked oligomer systems. Further, the formation of not only boron complexes but also other metal complexes based on the dipyrrolyldiketone framework is now under investigation.

Experimental section

General Procedures

Starting materials were purchased from Wako Chemical Co., Nacalai Chemical Co., and Aldrich Chemical Co. and used without further purification unless otherwise stated. UV-visible spectra were recorded on a Hitachi U-3500 spectrometer. Fluorescence spectra and quantum yields were recorded on a Hitachi F-4500 fluorescence spectrometer and a Hamamatsu Quantum Yields Measurements System for Organic LED Materials C9920-02, respectively. NMR spectra used in the characterization of products were recorded on a JEOL ECA-600 600 MHz spectrometers. All NMR spectra were referenced to solvent. Matrix-assisted laser desorption ionization time-of-flight mass spectrometries (MALDI-TOF-MS) were recorded on a Shimadzu Axima-CFRplus using positive mode. TLC analyses were carried out on aluminium sheets coated with silica gel 60 (Merck 5554). Column chromatography was performed on Sumitomo alumina KCG-1525, Wakogel C-200, C-300, and Merck silica gel 60 and 60H.

Catechol-substituted boron complex of 1,3-bis(3,4-diethyl-5-iodopyrrol-2-yl)-1,3-propanedione, 2b-I_2

Following the literature procedure,[5b] to a CH_2Cl_2 (35 mL) solution of **2b**[6] (130.3 mg, 0.30 mmol) at room temperature was added *N*-iodosuccinimide (165.0 mg, 0.72 mmol). The mixture was stirred at 0 °C for 6.5 h. After confirming the consumption of the starting material by TLC analysis, the mixture was washed with water and extracted with CH_2Cl_2, dried over anhydrous Na_2SO_4, and evaporated to dryness. The residue was then chromatographed over a silica gel flash column (eluent: 20% hexane–CH_2Cl_2) and recrystallized from CH_2Cl_2–hexane to afford bisiodo-substituted **2b-I_2** (27 mg, 13%) as a red solid. R_f 0.65 (CH_2Cl_2). ^{1}H NMR (600 MHz, $CDCl_3$, 20 °C): δ (ppm) 9.39 (m, 2H, NH), 6.86 (m, 2H, catechol-H), 6.80 (m, 2H, catechol-H), 6.43 (s, 1H, CH), 2.80 (m, 4H, CH_2), 2.48 (m, 4H, CH_2), 1.27 (m, 6H, CH_3), 1.21 (m, 6H, CH_3). UV/vis (CH_2Cl_2, λ_{max}[nm] (ε, 10^5 $M^{-1}cm^{-1}$)): 481.0 (1.14). MALDI-TOF-MS: *m/z* (% intensity): 684.0 (100), 685.0 (70), 686.0 (32). Calcd for $C_{25}H_{27}BI_2N_2O_4$ ($[M]^+$): 684.02.

Catechol-substituted boron complex of 1,3-(5-phenylpyrrol-2-yl)-1,3-propanedione, 2c

A dry CH_2Cl_2 solution (30 mL) of 1,3-di-(5-phenylpyrrol-2-yl)-1,3-propanedione[5a] (9.61 mg, 0.027 mmol) was treated with a CH_2Cl_2 solution (0.27 mL) of BCl_3 (0.265 mg, 0.27 mmol) in at room temperature under nitrogen and was stirred for 2 h at the same temperature. The mixture became red. After the consumption of starting diketone was confirmed by TLC analysis, catechol (3.85 mg, 0.035 mmol) was added. After 3 h, the mixture was washed with Na_2CO_3 aq. and water, dried over anhydrous Na_2SO_4, filtered, and evaporated to dryness. The residue was then chromatographed over a silica gel column (eluent: CH_2Cl_2) and recrystallized from CH_2Cl_2–hexane to afford **2c** (10.2 mg, 80%) as a red solid. R_f 0.43 (2% MeOH–CH_2Cl_2). ^{1}H NMR (600 MHz, $CDCl_3$, 20 °C): δ (ppm) 9.62 (m, 2H, NH), 7.61 (m, 4H, Ar–H), 7.43 (m, 4H, Ar–H), 7.36 (m, 2H, Ar–H), 7.25 (m, 2H, pyrrole-H), 6.96 (m, 2H, catechol-H), 6.82 (m, 2H, catechol-H), 6.74 (m, 2H, pyrrole-H), 6.62 (s, 1H, CH). UV/vis (CH_2Cl_2, λ_{max}[nm] (ε, 10^5 $M^{-1}cm^{-1}$)): 503.0 (1.08). MALDI-TOF-MS: *m/z* (% intensity): 471.2 (24), 472.2 (100), 473.2 (50). Calcd for $C_{29}H_{21}BN_2O_4$ ($[M]^+$): 472.16.

Catechol-substituted boron complex of 1,3-bis(3,4-diethyl-5-phenylpyrrol-2-yl)-1,3-propanedione, 2d

A two necked flask containing **2b-I_2** (10.2 mg, 0.015 mmol), phenylboronic acid (4.5 mg, 0.037 mmol), tetrakis(triphenylphosphine)palladium(0) (4.1 mg, 0.0035 mmol), and Na_2CO_3 (12.5 mg, 0.12 mmol) was flushed with nitrogen and charged with a mixture of degassed 1,2-dimethoxyethane (1 mL), and water (0.1 mL). The mixture was heated at 80 °C for 18 h, cooled, then partitioned between water and CH_2Cl_2. The combined extracts were dried over anhydrous Na_2SO_4 and evaporated. The residue was then chromatographed over a silica gel column (eluent: 10% hexane–CH_2Cl_2) and recrystallized from CH_2Cl_2–hexane to afford **2d** (2.3 mg, 27%) as a red solid. R_f 0.53 (10% hexane–CH_2Cl_2). ^{1}H NMR (600 MHz, $CDCl_3$, 20 °C): δ (ppm) 9.35 (m, 2H, NH), 7.49 (d, J = 7.8 Hz, 4H, phenyl-H), 7.43 (t, J = 7.8 Hz, 4H, phenyl-H), 7.37 (d, J = 7.8 Hz, 2H,

phenyl-H), 6.83 (m, 2H, catechol-H), 6.76 (m, 2H, catechol-H), 6.64 (s, 1H, CH), 2.88 (q, J = 7.8 Hz, 4H, CH_2), 2.62 (q, J = 7.8 Hz, 4H, CH_2), 1.37 (t, J = 7.8 Hz, 6H, CH_3), 1.19 (t, J = 7.8 Hz, 6H, CH_3). UV/vis (CH_2Cl_2, λ_{max}[nm] (ε, 10^5 $M^{-1}cm^{-1}$)): 502.0 (1.10). MALDI-TOF-MS: m/z (% intensity): 583.2 (35), 584.2 (100), 585.2 (72). Calcd for $C_{37}H_{37}BN_2O_4$ ($[M]^+$): 584.28. This compound was further characterized by X-ray diffraction analysis.

Diphenyl-substituted boron complex of 1,3-dipyrrol-2-yl-1,3-propanedione, 3a

BPh_3 (73.3 mg, 0.30 mmol) was added to a solution of 1,3-dipyrrol-2-yl-1,3-propanedione[4a] (20.0 mg, 0.099 mmol) in dry toluene (3.0 mL) under nitrogen and was refluxed for 14 h. The solvent was evaporated to dryness. The residue was then chromatographed over a silica gel flash column (eluent: CH_2Cl_2) and recrystallized from CH_2Cl_2–hexane to afford **3a** (25.6 mg, 71%) as a yellow solid. R_f 0.67 (CH_2Cl_2). ^{1}H NMR (600 MHz, $CDCl_3$, 20 °C): δ (ppm) 9.52 (m, 2H, NH), 7.49 (d, J = 7.8 Hz, 4H, phenyl-H), 7.24 (m, 6H, phenyl-H), 7.12 (m, 2H, pyrrole-H), 7.05 (m, 2H, pyrrole-H), 6.38 (s, 1H, CH), 6.37 (m, 2H, pyrrole-H). UV/vis (CH_2Cl_2, λ_{max}[nm] (ε, 10^5 $M^{-1}cm^{-1}$)): 435.0 (0.75). MALDI-TOF-MS: m/z (% intensity): 365.1 (16), 366.1 (100), 367.1 (94). Calcd for $C_{31}H_{35}BN_2O_2$ ($[M]^+$): 366.15. This compound was further characterized by X-ray diffraction analysis.

Diphenyl-substituted boron complex of 1,3-bis-(3,4-diethylpyrrol-2-yl)-1,3-propanedione, 3b

BPh_3 (297.7 mg, 1.25 mmol) was added to a solution of 1,3-bis-(3,4-diethylpyrrol-2-yl)-1,3-propanedione[4b] (55.5 mg, 0.25 mmol) in dry toluene (3.5 mL) under nitrogen and was refluxed for 12 h. The solvent was evaporated to dryness. The residue was then chromatographed over a silica gel flash column (eluent: 50% hexane–CH_2Cl_2) and recrystallized from CH_2Cl_2–hexane to afford **3b** (78.4 mg, 66%) as a yellow solid. R_f 0.33 (50% hexane–CH_2Cl_2). ^{1}H NMR (600 MHz, $CDCl_3$, 20 °C): δ (ppm) 9.31 (m, 2H, NH), 7.51 (d, J = 7.8 Hz, 4H, phenyl-H), 7.22 (m, 6H, phenyl-H), 6.88 (d, J = 3.0 Hz, 2H, pyrrole-H), 6.37 (s, 1H, CH), 2.77 (q, J = 7.8 Hz, 4H, CH_2), 2.47 (q, J = 7.8 Hz, 4H, CH_2), 1.22 (m, 12H, CH_3). UV/vis (CH_2Cl_2, λ_{max}[nm] (ε, 10^5 $M^{-1}cm^{-1}$)): 448.0 (0.93). MALDI-TOF-MS: m/z (% intensity): 477.2 (82), 478.2 (100), 479.2 (37). Calcd for $C_{31}H_{35}BN_2O_2$ ($[M]^+$): 478.28. This compound was further characterized by X-ray diffraction analysis.

Diphenyl-substituted boron complex of 1,3-bis(3,4-diethyl-5-iodopyrrol-2-yl)-1,3-propanedione, 3b-I_2

Following the literature procedure,[5b] to a CH_2Cl_2 (60 mL) solution of **3b** (197.3 mg, 0.41 mmol) at room temperature was added *N*-iodosuccinimide (257.4 mg, 1.1 mmol). The mixture was stirred at room temperature for 3 h. After confirming the consumption of the starting material by TLC analysis, the mixture was washed with water and extracted with CH_2Cl_2, dried over anhydrous Na_2SO_4, and evaporated to dryness. The residue was then chromatographed over a silica gel flash column (eluent: 50% hexane–CH_2Cl_2) and recrystallized from CH_2Cl_2–hexane to afford **3b-I_2** (193.8 mg, 64%) as an orange solid. R_f 0.35 (50% hexane–CH_2Cl_2). ^{1}H NMR (600 MHz, $CDCl_3$, 20 °C): δ (ppm) 9.38 (m, 2H, NH), 7.50 (d, J = 8.4 Hz, 4H, phenyl-H), 7.30 (d, J = 7.2 Hz, 4H, phenyl-H), 7.25 (m, 2H, phenyl-H), 6.26 (s, 1H, CH), 2.77 (q, J = 7.8 Hz, 4H, CH_2), 2.42 (q, J = 7.8 Hz, 4H, CH_2), 1.22 (t, J = 7.8 Hz, 6H, CH_3), 1.09 (t, J = 7.8 Hz, 6H, CH_3). UV/vis (CH_2Cl_2, λ_{max}[nm] (ε, 10^5 $M^{-1}cm^{-1}$)): 470.0 (1.21). MALDI-TOF-MS: m/z (% intensity): 729.1 (35), 730.1 (100), 731.1 (50). Calcd for $C_{31}H_{33}BI_2N_2O_2$ ($[M]^+$): 730.07. This compound was further characterized by X-ray diffraction analysis.

Diphenyl-substituted boron complex of 1,3-(5-phenylpyrrol-2-yl)-1,3-propanedione, 3c

BPh_3 (74.1 mg, 0.33 mmol) was added to a solution of 1,3-di-(5-phenylpyrrol-2-yl)-1,3-propanedione[5a] (35.0 mg, 0.099 mmol) in dry toluene (2.5 mL) under nitrogen and was refluxed for 12 h. The solvent was evaporated to dryness. The residue was then chromatographed over silica gel flash column (eluent: 50% hexane–CH_2Cl_2) and recrystallized from CH_2Cl_2–hexane to afford **3c** (33.6 mg, 66%) as an orange solid. R_f 0.30 (50% hexane–CH_2Cl_2). ^{1}H NMR (600 MHz, $CDCl_3$, 20 °C): δ (ppm) 9.64 (m, 2H, NH), 7.64 (d, J = 7.8 Hz, 4H, phenyl-H), 7.58 (d, J = 7.2 Hz, 4H, phenyl-H), 7.45 (t, J = 7.8 Hz, 4H, phenyl-H), 7.36 (t, J = 7.8 Hz, 2H, phenyl-H), 7.30 (t, J = 7.2 Hz, 4H, phenyl-H), 7.26 (m, 2H, phenyl-H), 7.12 (m, 2H, pyrrole-H), 6.69 (m, 2H, pyrrole-H), 6.46 (s, 1H, CH). UV/vis (CH_2Cl_2, λ_{max}[nm] (ε, 10^5 $M^{-1}cm^{-1}$)): 492.0 (1.38). MALDI-TOF-MS: m/z (% intensity): 518.2 (100), 519.2 (62), 520.2 (27). Calcd for $C_{35}H_{27}BN_2O_2$ ($[M]^+$): 518.22. This compound was further characterized by X-ray diffraction analysis.

Diphenyl-substituted boron complex of 1,3-bis(3,4-diethyl-5-phenylpyrrol-2-yl)-1,3-propanedione, 3d

A two necked flask containing **3b-I_2** (190.8 mg, 0.26 mmol), phenylboronic acid (70.7 mg, 0.58 mmol), tetrakis(triphenylphosphine)palladium(0) (54.3 mg, 0.050 mmol), and Na_2CO_3 (205.0 mg, 1.9 mmol) was flushed with nitrogen and charged with a mixture of degassed 1,2-dimethoxyethane (12 mL), and water (1.2 mL). The mixture was heated at 80 °C for 18 h, cooled, then partitioned between water and CH_2Cl_2. The combined extracts were dried over anhydrous Na_2SO_4 and evaporated. The residue was then chromatographed over silica gel column (eluent: 50% hexane–CH_2Cl_2) and recrystallized from CH_2Cl_2–hexane to afford **3d** (22.7 mg, 14%) as an orange solid. R_f 0.45 (10% hexane–CH_2Cl_2). ^{1}H NMR (600 MHz, $CDCl_3$, 20 °C): δ (ppm) 9.29 (m, 2H, NH), 7.54 (d, J = 7.8 Hz, 4H, phenyl-H), 7.48 (m, 8H, phenyl-H), 7.39 (t, J = 7.2 Hz, 2H, phenyl-H), 7.27 (m, 4H, phenyl-H), 7.21 (t, J = 7.2 Hz, 2H, phenyl-H), 6.47 (s, 1H, CH), 2.85 (q, J = 7.8 Hz, 4H, CH_2), 2.62 (q, J = 7.8 Hz, 4H, CH_2), 1.32 (t, J = 7.8 Hz, 6H, CH_3), 1.19 (t, J = 7.8 Hz, 6H, CH_3). UV/vis (CH_2Cl_2, λ_{max}[nm] (ε, 10^5 $M^{-1}cm^{-1}$)): 489.0 (1.01). MALDI-TOF-MS: m/z (% intensity): 629.3 (11), 630.3 (100), 631.3 (21). Calcd for $C_{43}H_{43}BN_2O_4$ ($[M]^+$): 630.34. This compound was further characterized by X-ray diffraction analysis.

Method for X-ray analysis

Crystallographic data are summarised in Table 3. A single crystal of **2d** was obtained by vapour diffusion of octane into a CH_2Cl_2 solution of **2d**. The data crystal was a red prism of approximate

Table 3 Crystallographic details for anion receptors and anion complexes

	2d	**3a**	**3b**	**3b-I_2**	**3c**	**3c**·acetone$_2$	**3d**	**3a**·TBABr	**3b**·TBABr	**3c**·TBABr	**3d**·TBACl
Formula	$C_{37}H_{37}BN_2O_4$	$C_{23}H_{19}BN_2O_2$	$C_{31}H_{35}BN_2O_2$	$C_{31}H_{33}BI_2N_2O_2$	$C_{35}H_{27}BN_2O_2\cdot CH_2Cl_2$	$C_{25}H_{27}BN_2O_2\cdot 2C_3H_6O$	$C_{43}H_{43}BN_2O_2$	$C_{23}H_{19}BN_2O_2\cdot C_{16}H_{36}NBr$	$C_{31}H_{35}BN_2O_2\cdot C_{16}H_{36}NBr$	$C_{35}H_{27}BN_2O_2\cdot C_{16}H_{36}NBr$	$C_{59}H_{78}BClN_3O_2$
FW	584.50	366.21	478.42	730.20	603.32	634.55	630.60	688.58	800.79	840.76	907.5335
Crystal size/mm	0.50 × 0.45 × 0.35	0.50 × 0.30 × 0.30	0.60 × 0.40 × 0.30	0.70 × 0.30 × 0.20	0.40 × 0.30 × 0.20	0.50 × 0.40 × 0.40	0.30 × 0.25 × 0.10	0.50 × 0.20 × 0.10	0.50 × 0.30 × 0.20	0.45 × 0.40 × 0.30	0.60 × 0.40 × 0.10
Crystal system	Triclinic	Monoclinic	Orthorhombic	Triclinic	Triclinic	Monoclinic	Triclinic	Monoclinic	Triclinic	Monoclinic	Monoclinic
Space group	$P\bar{1}$ (no. 2)	$P2_1/n$ (no. 14)	$Pcca$ (no. 54)	$P\bar{1}$ (no. 2)	$P\bar{1}$ (no. 2)	$P2_1/n$ (no. 14)	$P\bar{1}$ (no. 2)	$P2_1$ (no. 4)	$P\bar{1}$ (no. 2)	$P2_1/c$ (no. 14)	$P2_1$ (no. 4)
a/Å	9.420(4)	11.512(5)	22.300(9)	9.575(3)	11.615(4)	10.102(2)	9.827(4)	12.662(3)	9.031(2)	13.723(3)	8.475(3)
b/Å	12.575(5)	14.056(4)	17.053(8)	16.463(6)	13.859(5)	18.284(5)	11.506(3)	16.559(3)	13.255(5)	14.488(2)	23.006(6)
c/Å	14.778(6)	11.554(4)	21.385(7)	19.426(5)	20.323(7)	18.278(4)	15.784(5)	19.055(4)	19.555(6)	23.592(5)	13.458(3)
α (°)	70.802(18)	90	90	97.835(12)	73.013(14)	90	78.919(11)	90	96.453(13)	90	90
β (°)	82.598(16)	99.314(16)	90	100.782(11)	79.998(12)	95.046(10)	88.635(14)	107.376(9)	90.315(11)	103.643(8)	98.080(10)
γ (°)	67.874(15)	90	90	98.801(14)	79.432(14)	90	77.553(13)	90	106.498(11)	90	90
V/Å^3	1531.4(11)	1844.9(12)	8132(6)	2929.3(16)	3050.5(19)	3363.1(14)	1710.0(10)	3813.0(13)	2228.6(12)	4558.3(16)	2598.2(12)
ρ_c/g cm^{-3}	1.268	1.318	1.172	1.656	1.314	1.253	1.225	1.199	1.193	1.225	1.161
Z	2	4	12	4	4	4	2	4	2	4	2
T/K	123(2)	123(2)	296(2)	123(2)	123(2)	123(2)	123(2)	123(2)	123(2)	123(2)	123(2)
μ(Mo-Kα)/mm^{-1}	0.082	0.084	0.072	2.178	0.249	0.080	0.074	1.113	0.962	0.944	0.118
no. of reflns	10363	17717	42895	28712	29747	32199	16251	36595	15048	38565	25671
no. of unique reflns	4518	4211	9064	13289	13828	7684	7743	17049	6516	8931	11812
variables	401	253	494	733	803	437	437	837	516	551	603
$\lambda_{\text{Mo-K}\alpha}$, Å	0.71075	0.71075	0.71075	0.71075	0.71075	0.71075	0.71075	0.71075	0.71075	0.71075	0.71075
R_1 ($I > 2\sigma(I)$)	0.0470	0.0403	0.0855	0.0308	0.0448	0.0445	0.0536	0.0737	0.0631	0.1291	0.0441
wR_2 ($I > 2\sigma(I)$)	0.1553	0.1029	0.1428	0.0772	0.1219	0.1032	0.1221	0.1593	0.1646	0.3975	0.0957
GOF	1.340	1.037	1.048	1.053	0.906	1.067	1.053	1.026	1.165	1.795	1.039

dimensions 0.50 mm × 0.45 mm × 0.35 mm. Data were collected at 123 K on a Rigaku RAXIS-RAPID diffractometer with graphite monochromated Mo-Kα radiation (λ = 0.71075 Å), structure was solved by direct methods. A single crystal of **3a** was obtained by vapor diffusion of hexane into a CH_2Cl_2 solution of **3a**. The data crystal was a yellow prism of approximate dimensions 0.50 mm × 0.30 mm × 0.30 mm. Data were collected at 123 K on a Rigaku RAXIS-RAPID diffractometer with graphite monochromated Mo-Kα radiation (λ = 0.71075 Å), structure was solved by direct methods. A single crystal of **3b** was obtained by vapour diffusion of hexane into a CH_2Cl_2 solution of **3b**. The data crystal was a yellow prism of approximate dimensions 0.60 mm × 0.40 mm × 0.30 mm. Data were collected at 296 K on a Rigaku RAXIS-RAPID diffractometer with graphite monochromated Mo-Kα radiation (λ = 0.71075 Å), structure was solved by direct methods. A single crystal of **3b-I$_2$** was obtained by vapour diffusion of hexane into a CH_2Cl_2 solution of **3b-I$_2$**. The data crystal was a pink prism of approximate dimensions 0.70 mm × 0.30 mm × 0.20 mm. Data were collected at 123 K on a Rigaku RAXIS-RAPID diffractometer with graphite monochromated Mo-Kα radiation (λ = 0.71075 Å), structure was solved by direct methods. A single crystal of **3c** was obtained by vapour diffusion of hexane into a CH_2Cl_2 solution of **3c**. The data crystal was a red prism of approximate dimensions 0.40 mm × 0.30 mm × 0.20 mm. Data were collected at 123 K on a Rigaku RAXIS-RAPID diffractometer with graphite monochromated Mo-Kα radiation (λ = 0.71075 Å), structure was solved by direct methods. A single crystal of **3c**·acetone$_2$ was obtained by vapour diffusion of hexane into an acetone solution of **3c**. The data crystal was an orange prism of approximate dimensions 0.50 mm × 0.40 mm × 0.40 mm. Data were collected at 123 K on a Rigaku RAXIS-RAPID diffractometer with graphite monochromated Mo-Kα radiation (λ = 0.71075 Å), structure was solved by direct methods. A single crystal of **3c** was obtained by vapour diffusion of hexane into a CH_2Cl_2 solution of **3d**. The data crystal was a yellow prism of approximate dimensions 0.30 mm × 0.25 mm × 0.10 mm. Data were collected at 123 K on a Rigaku RAXIS-RAPID diffractometer with graphite monochromated Mo-Kα radiation (λ = 0.71075 Å), structure was solved by direct methods. A single crystal of **3a**·TBABr was obtained by vapour diffusion of octane into EtOAc and CH_2Cl_2 solutions of **3a** and 1 equiv of TBABr. The data crystal was a yellow prism of approximate dimensions 0.50 mm × 0.20 mm × 0.10 mm. Data were collected at 123 K on a Rigaku RAXIS-RAPID diffractometer with graphite monochromated Mo-Kα radiation (λ = 0.71075 Å), structure was solved by direct methods. A single crystal of **3b**·TBABr was obtained by vapour diffusion of octane into EtOAc solution of **3b** and 1 equiv of TBABr. The data crystal was a yellow prism of approximate dimensions 0.50 mm × 0.30 mm × 0.20 mm. Data were collected at 123 K on a Rigaku RAXIS-RAPID diffractometer with graphite monochromated Mo-Kα radiation (λ = 0.71075 Å), structure was solved by direct methods. A single crystal of **3c**·TBABr was obtained by vapor diffusion of octane into EtOAc solution of **3c** and 1 equiv of TBABr. The data crystal was a yellow prism of approximate dimensions 0.45 mm × 0.40 mm × 0.30 mm. Data were collected at 123 K on a Rigaku RAXIS-RAPID diffractometer with graphite monochromated Mo-Kα radiation (λ = 0.71075 Å), structure was solved by direct methods. A single crystal of **3d**·TBACl was obtained by vapour diffusion of octane into EtOAc and CH_2Cl_2 solutions of **3d** and 1 equiv of TBACl. The data crystal was a yellow prism of approximate dimensions 0.60 mm × 0.40 mm × 0.10 mm. Data were collected at 123 K on a Rigaku RAXIS-RAPID diffractometer with graphite monochromated Mo-Kα radiation (λ = 0.71075 Å), structure was solved by direct methods. In each case, the non-hydrogen atoms were refined anisotropically. The calculations were performed using the Crystal Structure crystallographic software package of Molecular Structure Corporation.†

DFT Calculation

Ab initio calculations were carried out by using Gaussian 03 program[8] and an HP Compaq dc5100 SFF computer. The structures were optimized, and the total electronic energies were calculated at the B3LYP level using a 6-31G** basis set. Molecular orbitals were determined by single point calculations at the B3LYP level using a 6-31+G** basis set of the optimized structures at the B3LYP level using a 6-31G** basis set.

Acknowledgements

This work was supported by Grant-in-Aid for Young Scientists (B) (No. 21750155) and for Scientific Research in a Priority Area "Super-Hierarchical Structures" (No. 19022036) from the Ministry of Education, Culture, Sports, Science and Technology (MEXT) and Ritsumeikan Global Innovation Research Organization (R-GIRO) project (2008–2013). We thank Prof. Atsuhiro Osuka, Dr Shohei Saito, Mr Eiji Tsurumaki and Mr Taro Koide, Kyoto University, for X-ray analysis and Prof. Hitoshi Tamiaki, Ritsumeikan University, for various measurements.

Notes and references

1 (*a*) *Supramolecular Chemistry of Anions*, ed. A. Bianchi, K. Bowman-James and E. García-España, Wiley-VCH, New York, 1997; (*b*) *Fundamentals and Applications of Anion Separations*, ed. R. P. Singh and B. A. Moyer, Kluwer Academic/Plenum Publishers, New York, 2004; (*c*) *Anion Sensing*, ed. I. Stibor, *Topics in Current Chemistry*, Springer-Verlag, Berlin, 2005, 255, pp. 238; (*d*) P. A. J. L. SesslerP. A. Gale and W.-S. Cho, *Anion Receptor Chemistry*, RSC, Cambridge, 2006; (*e*) *Recognition of Anions*, ed. R. Vilar, *Structure and Bonding*, Springer-Verlag, Berlin, 2008.

2 (*a*) F. P. Schmidtchen and M. Berger, *Chem. Rev.*, 1997, **97**, 1609; (*b*) P. D. Beer and P. A. Gale, *Angew. Chem., Int. Ed.*, 2001, **40**, 486; (*c*) R. Martínez-Máñez and F. Sancenón, *Chem. Rev.*, 2003, **103**, 4419; (*d*) P. A. Gale and R. Quesada, *Coord. Chem. Rev.*, 2006, **250**, 3219; (*e*) P. Blondeau, M. Segura, R. Perez-Fernandez and J. de Mendoza, *Chem. Soc. Rev.*, 2007, **36**, 198; (*f*) P. A. Gale, S. E. García-Garrido and J. Garric, *Chem. Soc. Rev.*, 2008, **37**, 151; (*g*) C. Caltagirone and P. A. Gale, *Chem. Soc. Rev.*, 2009, **38**, 520.

3 (*a*) H. Maeda, *Eur. J. Org. Chem.*, 2007, 5313; (*b*) H. Maeda, *Chem. Eur. J.*, 2008, **14**, 11274; (*c*) H. Maeda, *J. Inclusion Phenom. Macrocyclic Chem.*, 2009, **64**, 193; (*d*) H. Maeda, in *Handbook of Porphyrin Science*, K. M. Kadish, K. M. Smith and R. Guilard, ed.; World Scientific, New Jersey, 2010, Vol. 8, Ch. 38.; (*e*) H. Maeda, in *Anion Complexation by Heterocycle Based Receptors, Topics in Heterocyclic Chemistry*, P. A. Gale and W. Dehaen, ed.; Springer-Verlag: Berlin, 2010, in press.

4 (*a*) H. Maeda and Y. Kusunose, *Chem. Eur. J.*, 2005, **11**, 5661; (*b*) H. Maeda, Y. Kusunose, Y. Mihashi and T. Mizoguchi, *J. Org. Chem.*, 2007, **72**, 2612; (*c*) H. Maeda, M. Terasaki, Y. Haketa, Y. Mihashi and Y. Kusunose, *Org. Biomol. Chem.*, 2008, **6**, 433.

5 (*a*) H. Maeda, Y. Haketa and T. Nakanishi, *J. Am. Chem. Soc.*, 2007, **129**, 13661; (*b*) H. Maeda and Y. Haketa, *Org. Biomol. Chem.*, 2008, **6**, 3091; (*c*) H. Maeda, Y. Mihashi and Y. Haketa, *Org. Lett.*, 2008, **10**, 3179; (*d*) H. Maeda, Y. Ito, Y. Haketa, N. Eifuku, E. Lee, M. Lee, T.

Hashishin and K. Kaneko, *Chem. Eur. J.*, 2009, **15**, 3709; (*e*) H. Maeda, Y. Terashima, Y. Haketa, A. Asano, Y. Honsho, S. Seki, M. Shimizu, H. Mukai and K. Ohta, *Chem. Commun.*, 2010, **46**(25), 4559–4561; (*f*) H. Maeda, Y. Bando, Y. Haketa, Y. Honsho, S. Seki, H. Nakajima and N. Tohnai, *Chem. Eur. J.*, 2010, DOI: 10.1002/chem.201001852.

6 H. Maeda, Y. Fujii and Y. Mihashi, *Chem. Commun.*, 2008, 4285.

7 A. Nagai, K. Kokado, Y. Nagata, M. Arita and Y. Chujo, *J. Org. Chem.*, 2008, **73**, 8605.

8 All calculations were carried out using the Gaussian 03 program; *Gaussian 03, Revision C.01*, M. J. Frisch, G. W. Trucks, H. B. Schlegel, G. E. Scuseria, M. A. Robb, J. R. Cheeseman, J. A. Montgomery, Jr., T. Vreven, K. N. Kudin, J. C. Burant, J. M. Millam, S. S. Iyengar, J. Tomasi, V. Barone, B. Mennucci, M. Cossi, G. Scalmani, N. Rega, G. A. Petersson, H. Nakatsuji, M. Hada, M. Ehara, K. Toyota, R. Fukuda, J. Hasegawa, M. Ishida, T. Nakajima, Y. Honda, O. Kitao, H. Nakai, M. Klene, X. Li, J. E. Knox, H. P. Hratchian, J. B. Cross, C. Adamo, J. Jaramillo, R. Gomperts, R. E. Stratmann, O. Yazyev, A. J. Austin, R. Cammi, C. Pomelli, J. W. Ochterski, P. Y. Ayala, K. Morokuma, G. A. Voth, P. Salvador, J. J. Dannenberg, V. G. Zakrzewski, S. Dapprich, A. D. Daniels, M. C. Strain, O. Farkas, D. K. Malick, A. D. Rabuck, K. Raghavachari, J. B. Foresman, J. V. Ortiz, Q. Cui, A. G. Baboul, S. Clifford, J. Cioslowski, B. B. Stefanov, G. Liu, A. Liashenko, P. Piskorz, I. Komaromi, R. L. Martin, D. J. Fox, T. Keith, M. A. Al-Laham, C. Y. Peng, A. Nanayakkara, M. Challacombe, P. M. W. Gill, B. Johnson, W. Chen, M. W. Wong, C. Gonzalez, and J. A. Pople, Gaussian, Inc., Wallingford CT, 2004.

9 A xenon lamp equipped with a light filter (>490 nm) was used for photooxidation of DPBF: A. N. Kozyref, V. Suresh, S. Das, M. O. Senge, M. Shibata, T. J. Dougherty and R. K. Pandey, *Tetrahedron*, 2000, **56**, 3353.